Available online at www.sciencedirect.com
ScienceDirect
Journal of the European Ceramic Society 27 (2007) 819–824
www.elsevier.com/locate/jeurceramsoc

Effect of Bi_2O_3 content on sintering and crystallization behavior of low-temperature firing Bi_2O_3–B_2O_3–SiO_2 glasses

Byung-Sook Kim, Eun-Sub Lim, Joon-Hyung Lee, Jeong-Joo Kim *

Department of Inorganic Materials Engineering, Kyungpook National University, Daegu 702-701, Republic of Korea

Available online 26 May 2006

Abstract

The sintering behavior of a Pb-free Bi_2O_3–B_2O_3–SiO_2 glass system was examined as a function of Bi_2O_3 content. The glass transition temperature and the crystallization temperature of the glasses decreased with different decreasing gradients as the Bi_2O_3 content increased. The change in temperature affected the sintering behaviors of the glasses. In the case of the 40 mol% Bi_2O_3 addition, large pore accompanied over-firing phenomenon was observed when the sample was sintered over the optimum sintering temperature. However, over-firing was not observed in the sample with 45 mol% of Bi_2O_3 because of the crystallized phases during sintering. When the Bi_2O_3 content was 50–55 mol%, the crystallization temperature became lower than the glass transition temperature, which resulted in the crystallization of glass and it hindered densification.

Keywords: Sintering; Glass; Over-firing; Low-temperature firing

1. Introduction

There has been an increase in interest regarding sintered glasses using amorphous powder as a raw starting material and their application to complex-shaped filters,[1,2] composites[3] and glass–ceramics.[4,5] In particular, significant developments in various electronic industries such as flat panel displays, low-temperature co-fired ceramics, and the packaging industry, need a variety of glass types, which can be easily densified at low temperatures.[6–8]

PbO-containing glass systems have become popular as commercial low temperature sinterable glass due to their high structural stability, low glass transition temperature and good thermal and electrical characteristics.[6,9] One of the advantages of PbO glasses is that they do not easily crystallize even when they contain 70% of PbO. This is because the PbO glass systems form PbO_4 structures easily since Pb plays the role of an intermediate due to its own ionic field strength.[10] However, recent environmental regulations have restricted the wide use of PbO systems, so the development of Pb-free or Pb-saving materials, which can replace PbO, has been undertaken. Bi_2O_3, BaO and ZnO have been employed as candidate materials that can replace PbO, particularly in the PbO–B_2O_3–SiO_2 system.[11–13] In this case, in order to obtain low glass transition temperatures, unlike the PbO glass system, a great amount of glass network modifier is necessary, thus resulting in devitrification and glass crystallization which affect glass properties and sintering behavior.[13,14]

It is well known that the sintering of glass materials is ruled by the mechanism of viscous flow, which is different from the diffusion mechanism of solid ceramics. Therefore, viscosity is one of the most important factors that can determine the sintering behavior of glasses.[15] If crystallization occurs during glass sintering, viscous flow is hindered. Depending upon the glass composition, crystallization occurs near the optimum sintering temperature (T_{sint}), at which maximum densification is obtained. When the crystallization temperature (T_c) of a glass is lower than the T_{sint}, densification does not occur because the crystallized phases lead to an infinite viscosity of the glass. When T_c is higher than T_{sint}, however, densification can occurs easily.[16–19]

In this study, the sintering behavior of Pb-free Bi_2O_3–B_2O_3–SiO_2 glasses was studied as a function of Bi_2O_3 content. The glass transition temperatures, the optimum sintering temperatures and the crystallization temperatures of the glasses were evaluated. The sintering behaviors of the glasses as a function of Bi_2O_3 content were discussed with respect to crystallization.

* Corresponding author. Tel.: +82 53 950 5635; fax: +82 53 950 5645.
E-mail address: jjkim@knu.ac.kr (J.-J. Kim).

0955-2219/$ – see front matter © 2006 Elsevier Ltd. All rights reserved.
doi:10.1016/j.jeurceramsoc.2006.04.013

Table 1
Experimental compositions of the Bi_2O_3–B_2O_3–SiO_2 glasses (mol%)

Designation	Bi_2O_3	B_2O_3	SiO_2
35Bi	35	35	30
40Bi	40	30	30
45Bi	45	25	30
50Bi	50	20	30
55Bi	55	15	30
60Bi	60	10	30

2. Experimental

High purity chemicals of Bi_2O_3 (Kojundo chemical lab Co., Ltd, 99.6%, Japan), H_3BO_3 (Kojundo chemical lab Co. Ltd., 99.9%, Japan), and SiO_2 (Kojundo chemical lab Co. Ltd., 99.9%, Japan) were used as starting raw materials. The amount of SiO_2 was fixed at 30 mol%, and the remaining 70 mol% was filled with Bi_2O_3 and B_2O_3, and the batch compositions employed are presented in Table 1.

The compositions are designated by the Bi_2O_3 content. Weighed raw powders were mixed in an alumina crucible for 15 min and melted at 1100 °C for 30 min in a Pt crucible. Then the molten glass in the crucible was dipped into cold water for quenching. The glass frit was roughly crushed in an alumina mortar and then planetary-milled (Pulverisette 6, Fritsch, Germany) for 2 h at 400 rpm. The crystallization of the glass powders was analyzed using an X-ray diffractometer (MO3-XHF, MAC Science Co., Japan). The density of the glass frits was measured using a gas-pycnometer. The glass transition temperature was measured using a DSC (Thermal Analyzer, DSC 2920, TA Instruments, USA) in the temperature range between room temperature and 650 °C at a heating rate of 5 °C/min. The glass powders were isostatically pressed under a pressure of 100 MPa for 3 min in order to form green pellets. The pellets were sintered in the temperature range between 430 and 470 °C at a 10 °C increments for 2 h at a heating rate of 5 °C/min and then the pellets were furnace cooled. The density of the sintered pellets was measured by the Archimedes method. The sintered pellets were broken by using a screw die and the fracture surface of the sintered samples was observed using a scanning electron microscope (JEOL, JSM-5400).

3. Results and discussion

The X-ray diffraction patterns of the Bi_2O_3–B_2O_3–SiO_2 glasses as a function of Bi_2O_3 content are presented in Fig. 1. A large broad peak around $2\theta = 25$–30 was observed in 25Bi–55Bi, which is a typical feature of borate glasses.[12] In the case of 60Bi, however, diffraction peaks appeared near 24°, 29° and 32°, which originated from Bi_2SiO_5 and $Bi_{45}BO_{69}$, signifying that the glass had crystallized. This is attributable to the devitrification of the 60Bi glass during the quenching process. Since the addition of Bi_2O_3 induces low viscosity of glasses due to the formation of non-bridging oxygen (NBO), devitrification might be viable in the 60Bi even if it was water-quenched. However, in the case of 35Bi, a phase separation occurred due to the immiscibility in the melt which resulted in an opaque glass.[20] Backscattered electron image observation, shown in Fig. 2, also supported the phase separation phenomenon. Therefore, the compositions of 60Bi and 35Bi will not be considered for further examination.

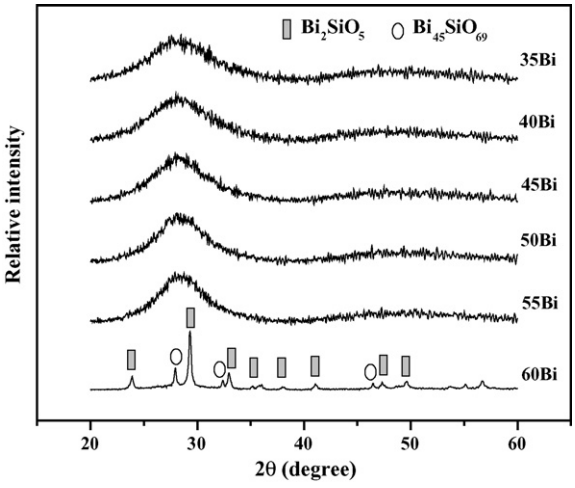

Fig. 1. XRD results of quenched compositions after melting at 1100 °C.

Fig. 3 shows the DSC results of the glasses except for Bi35 and Bi60. On the basis of the DSC curves, glass transition temperature (T_g) and crystallization temperature (T_C) values could be obtained.[21] In the case of T_g, three glass transition temperatures – the extrapolated onset temperature, the extrapolated end temperature and the mid temperature at which the heat capacity is midway between the extrapolated heat capacity of the liquid and glassy states – were evaluated. The mid glass transition temperature is indicated in Fig. 3 with plus (+) symbols. T_C was obtained by an extrapolation of the DSC curve at the deflection point where an exothermic peak begins to appear over the T_g. The T_C is indicated by triangle (△) symbols. In the case of the 40Bi–50Bi glasses, a small exothermic peak below T_C can be observed. This is considered to be the area where the fixed points such as T_{soft} (softening point) and T_{sint} (sintering temperature) appear between the T_g and T_C. The exact temperature of T_{soft} and T_{sint}, however, could not be determined from the DSC results. In the case of 55Bi, the T_C begins right after the T_g. It is found that the T_C and T_g decreased from 500 to 413.3 °C and from 430.4 to 387.5 °C, respectively, as a function of Bi_2O_3 content.

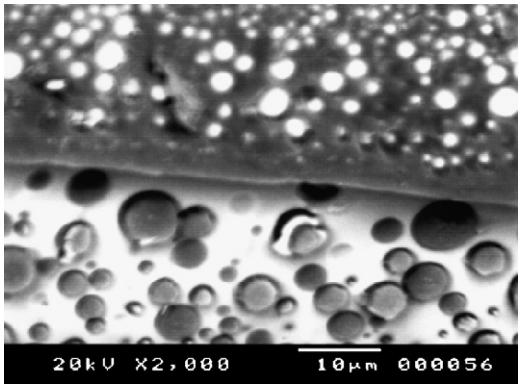

Fig. 2. BEI micrograph of the 35Bi glass after quenching.

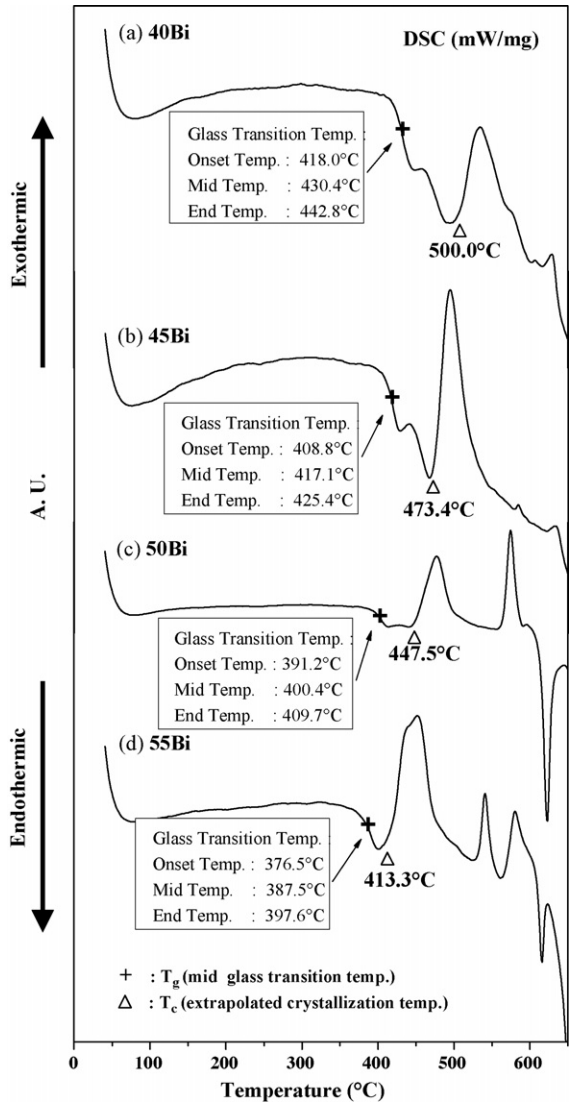

Fig. 3. DSC results of (a) 40Bi, (b) 45Bi, (c) 50Bi and (d) 55Bi as a function of temperature.

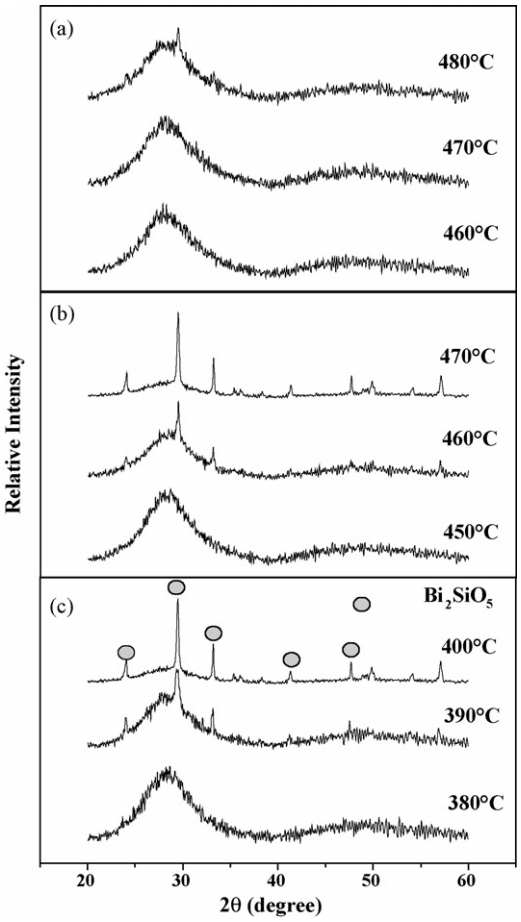

Fig. 4. XRD results of (a) 40Bi, (b) 45Bi and (c) 55Bi sintered at various temperatures.

This seems to be caused by the decrease in glass viscosity since Bi_2O_3 plays the role of network modifier.

Fig. 4 shows the X-ray diffraction patterns of specimens sintered at various temperatures for 2 h. The crystallization of the 40Bi glass started at 480 °C as shown in Fig. 4(a). As shown in Fig. 4(b) and (c), in glasses containing 45Bi and 55Bi, crystallization started at 460 and 390 °C, respectively. As the amount of Bi_2O_3 increased, the temperature where the crystallization was initiated decreased and the crystallized phase was Bi_2SiO_5 in every specimen.

Fig. 5 represents the T_g and T_C of the glasses as a function of Bi_2O_3 content. The T_{C1} obtained from the DSC and the T_{C2} obtained from the X-ray were differentiated in Fig. 5. The temperature at which sharp crystallization peaks appeared was regarded as the T_{C2} from the X-ray diffraction of the specimens, which were sintered for 2 h. The T_g, T_{C1} and T_{C2} decreased with the introduction of Bi_2O_3. The T_{C1} and T_{C2} show almost the same decreasing gradients. Since the gradient of T_g is smaller than those of the T_{CS} (T_{C1} and T_{C2}), the temperature gap between the T_g and T_{CS} for 40Bi is greater than that for 55Bi. This is believed to be caused by the different thermal histories of the glass samples between DSC and X-ray measurements as described in the experimental procedure.

Fig. 6 shows the relative density of specimens sintered at various temperatures. In the case of the 40Bi sample, density

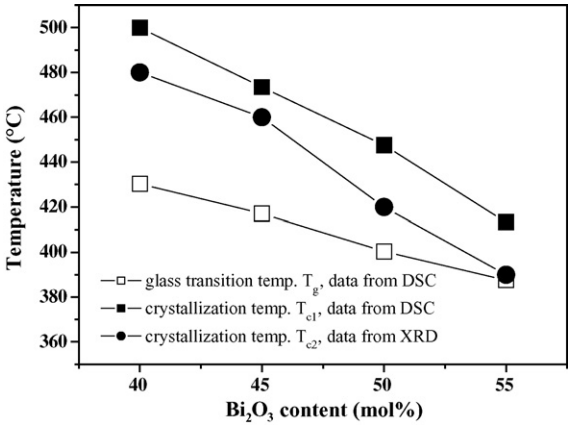

Fig. 5. Glass transition temperature (T_g) and crystallization temperature (T_C) of the glasses obtained from the DSC and X-ray analysis.

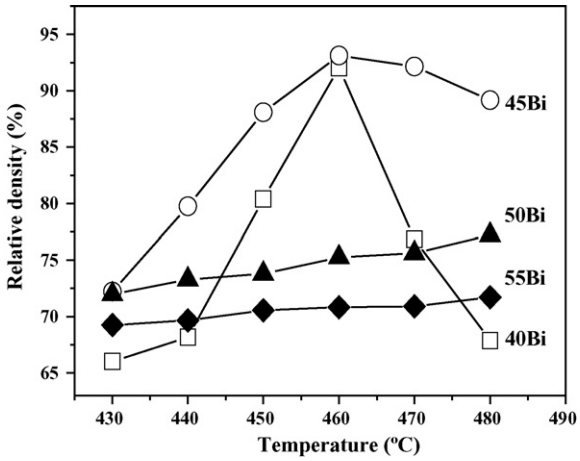

Fig. 6. Relative densities of the glass samples after sintering at various temperatures.

increased as the sintering temperature increased and maximum densification was attained at 460 °C. However, when the specimen was sintered above the optimum sintering temperature (T_{sint}) where maximum densification was attained, the density of the specimen dramatically decreased. This is the so-called over-firing phenomenon.[22] The 45Bi sample also showed maximum densification at 460 °C. However, a rapid decrease in density was not observed in the 45Bi. On the contrary, remarkable densification was not apparent in 50Bi and 55Bi even though the sintering temperature increased to 470 °C. This is caused by early crystallization before densification is initiated. Since the sintering of glass materials is ruled by the mechanism of viscous flow, crystallization during sintering hinders viscous flow. That is, when crystallization occurs first at a lower sintering temperature before densification has started, sintering is retarded due to the steep increase in glass viscosity. The 50Bi and 55Bi samples are such cases, i.e. the T_C is very close to the T_g and crystallization occurs below T_{soft} and T_{sint}.

Fig. 7 shows a fracture surface SEM image of the 40Bi, 45Bi and 55Bi samples sintered at 460 °C and 470 °C. Fig. 7(a) and (d) corresponds to the 40Bi sample, (b)–(e) correspond to the 45Bi sample and (c) and (f) correspond to the 55Bi sample. Note that the 40Bi sample did not crystallize during the whole sintering process, while the crystallization for 45Bi was initiated at the T_{sint}. In the 55Bi sample, crystallization occurred right after the T_g. Fig. 7(a) shows the microstructure of the 40Bi sample, which was sintered at its T_{sint}. Crystallization did not occur and a smooth fracture surface with fine isolated pores, which is a typical feature of glass, could be observed after sintering. However, increasing the temperature above its T_{sint} gave rise to the formation of large pores, as shown in Fig. 7(d). This caused a decrease in the relative density due to the over-firing phenomenon, as shown in Fig. 6. Fig. 7(b) shows the microstructure of the 45Bi sample, which was sintered at its T_{sint} and (e) was sintered at a temperature 10 °C higher than the T_{sint}. Rough surfaces were observed in (b) and (e) due to the crystallized phases. Fig. 7(c) and (e) shows the microstructures of the 55Bi samples sintered at 460 and 470 °C, respectively. Crystallized phases can be seen on the fracture surface of 55Bi and densification had not yet been initiated due to crystallization.

A schematic diagram, which explains the sintering behavior in relation to the T_g, T_{sint} and T_c, is shown in Fig. 8. Fig. 8(a)–(c) shows the sintering behavior of 40Bi, 45Bi and 55Bi, respectively. Fig. 8(a) shows a case whereby T_c is higher than T_{sint} and T_g. In this instance, maximum densification can be obtained at the T_{sint} and the over-firing phenomenon occurred when sintering was conducted above the T_{sint}. Increasing the temperature above the T_{sint} generates gas in the sample, as well as causing the coalescence and expansion of pores that lead to the formation of large pores, as shown in Fig. 7(d). As the temperature increases, the small pores can easily move to coalesce with the adjacent pores and grow to large pores because the viscosity of the glass decreases with an increase in temperature. When pore coalescence occurs, it results in an increase in the pore radius and a decrease in pore pressure. Therefore, the pore volume after coalescence is larger than the sum of the pore volumes before coalescence, which led to the generation of macro pores.[23] Fig. 8(b) shows a case where the T_c and T_{sint} are nearly

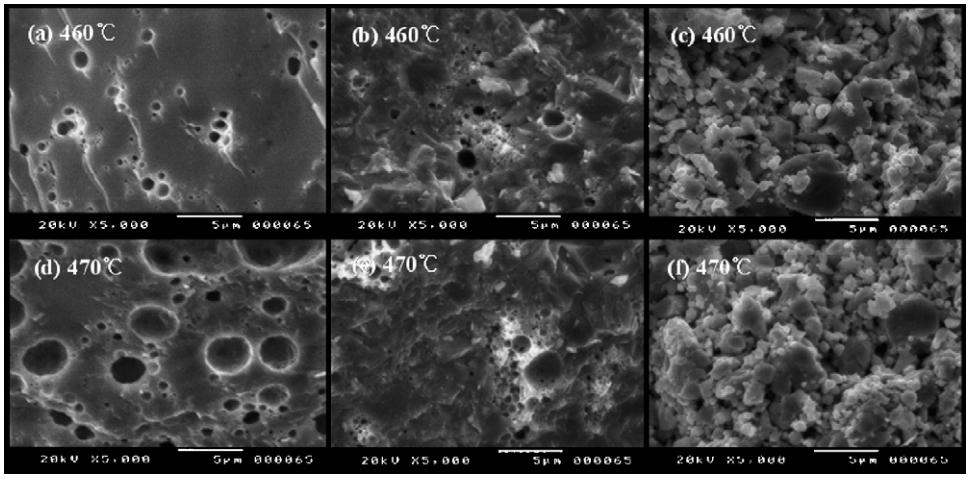

Fig. 7. SEM photographs of 40Bi (a) and (d), 45Bi (b) and (e), and 55Bi (c) and (f) sintered at different temperatures.

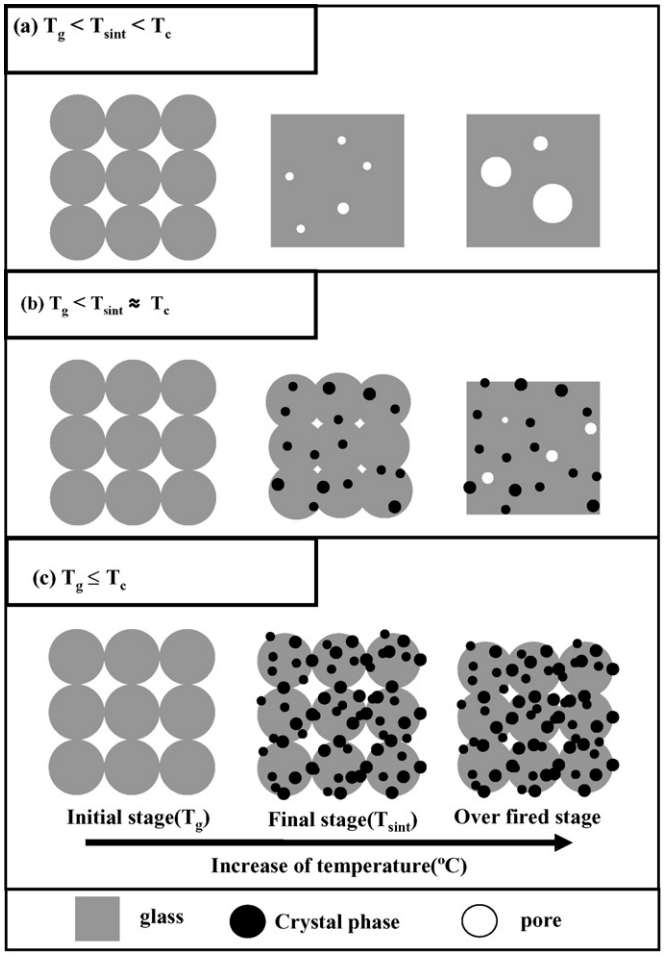

Fig. 8. Schematic diagram for the explanation of the sintering behaviors for (a) 40Bi, (b) 45Bi and (c) 55Bi in relation to T_g, T_{sint} and T_c.

the same, whereby densification and crystallization occur concurrently. Therefore, because of the increased viscosity due to the crystallized phases, the movement of isolated pores is difficult even at higher temperatures, thus inhibiting the over-firing phenomenon. When the T_C is located right after the T_g and crystallization occurs prior to densification as shown in Fig. 8(c), the viscosity of the glass drastically increases with the formation of the crystalline solid phase, which results in the retardation of sintering as shown in (c).

4. Conclusions

The current study examined the effect of Bi_2O_3 content on the sintering and crystallization behavior of the Pb-free low-temperature firing Bi_2O_3–B_2O_3–SiO_2 glass. A phase separation was observed due to immiscibility in the melt of the 35Bi and devitrification occurred in the 60Bi sample. Both the T_g and T_c decreased as the Bi_2O_3 content increased. However, the T_c showed a steeper gradient than the T_g with respect to the Bi_2O_3 content. This resulted in the different sintering behaviors of the glasses. When the T_c was higher than the T_{sint}, the sample was well-densified at the T_{sint}, and the over-firing phenomenon occurred at a sintering temperature over the T_{sint}. When the T_{sint} was higher than the T_g, and the T_{sint} and T_C were about the same, crystallization and densification progressed at the same time. However, when the T_c is located in the vicinity of the T_g (right after the T_g) the crystallized phases remained as they were without densification.

Acknowledgements

This work was supported by the National Research Laboratory grant from the Ministry of Science and Technology (MOST) and Korea Science and Engineering Foundation (KOSEF).

References

1. Ingelheim, M. S. and Kiefer, W., Ein “Glasschwamm” als Flussig keitsspeicher. *Schott Inform.*, 1983, **1**, 7–10.
2. Siebers, F. B., Greulich, N. and Kiefer, W., Manufacture, properties and application of open-pore sintered glasses and open-pore sintered glass–ceramics. *Glastech. Ber.*, 1989, **62**, 63–73.
3. Gong, W. L., Lutze, W. and Ewing, R. C., Reaction sintered glass: a durable matrix for spinel-forming nuclear waste compositions. *J. Nucl. Mater.*, 2000, **278**, 77–84.
4. Partridge, G., Nucleation and crystallisation phenomena in low expansion Li_2O–Al_2O_3–SiO_2 glass ceramics. *Glass Technol.*, 1982, **23**, 133–138.
5. Wang, M. L. and Stevens, R., Effects of microstructure on the colour variation of transparent glass ceramics. *Glass Technol.*, 1982, **23**, 139–145.
6. Hwang, G. H., Kim, W. Y., Jeon, H. J. and Kim, Y. S., Physical properties of barrier ribs of plasma display panels. Part II. Effects of fillers. *J. Am. Ceram. Soc.*, 2002, **85**, 2961–2964.
7. Kim, H. J., Chung, Y. S. and Auh, K. H., Development of transparent dielectric paste for PDP. *J. Korean Assoc. Cryst. Growth*, 1999, **9**, 50–54.
8. Pascual, M. J., Duran, A. and Pascual, L., Sintering process of glasses in the system Na_2O–B_2O_3–SiO_2. *J. Non-Cryst. Solids*, 2002, **306**, 58–69.
9. Hwang, G. H., Jeon, H. J. and Kim, Y. S., Physical properties of barrier ribs of plasma display panels. Part I. Formation of pores during sintering of lead borosilicate glass frits. *J. Am. Ceram. Soc.*, 2002, **85**, 2956–2960.
10. Scholze, *Glass: Nature, Structure and Properties*. Springer–Verlag, New York, 1991, pp. 5–8 (translated by Michael J. Lakin).
11. Jin, Y. H., Jeon, Y. W., Lee, B. C. and Ryu, B. K., Properties and structure of Bi_2O_3–B_2O_3-ZnO glasses for application in plasma display panels rib. *J. Korean Ceram. Soc.*, 2002, **39**, 184–189.
12. Lee, C. S., Yoo, J. R., Jung, K. W. and Choi, S. C., Fabrication of Pb free solder glass for electronic packaging application. *J. Korean Ceram. Soc.*, 2001, **38**, 628–633.
13. Kim, D. N., Lee, J. Y., Huh, J. S. and Kim, H. S., Thermal and electrical properties of BaO–B_2O_3–ZnO glasses. *J. Non-Cryst. Solids*, 2002, **306**, 70–75.
14. Kim, B. S., Kim, Y. N., Lim, E. S., Lee, J. H. and Kim, J. J., Effect of Al_2O_3 filler addition on sintering behavior and physical characteristics of BaO–B_2O_3–ZnO glass ceramic system. *J. Korean Ceram. Soc.*, 2005, **42**, 110–116.
15. Clasen, R., Preparation of high-purity silica glass by sintering of colloidal particles. *Glastech. Ber.*, 1987, **60**, 125–132.
16. Kim, J. S. and Cheon, C. I., Crystallization and void formation in ZnO–B_2O_3–SiO_2–MgO sintered solder glasses. *J. Mater. Sci.*, 1997, **32**, 1575–1579.
17. Pardo, M. O. and Zanotto, E. D., Glass sintering with concurrent crystallization. *C. R. Chim.*, 2002, **5**, 773–786.
18. Yon, S. J., Glass–ceramics of Li_2O–Al_2O_3–SiO_2 system produced by sintering. *J. Korean Assoc. Cryst. Growth*, 1993, **3**, 176–184.

19. Park, Y. W. and Hyun, B. S., Studies on the sintering of the cordierite glass–ceramics. *J. Korean Ceram. Soc.*, 1992, **29**, 779–784.
20. Zhao, P., Kroker, S. and Stebbins, J. F., Non-bridging oxygen sites in barium borosilicate glasses: results from ^{11}B and ^{17}O NMR. *J. Non-Cryst. Solids*, 2000, **276**, 122–131.
21. Klaus, H., Thermal analysis of glass. *Thermochim. Acta*, 1987, **110**, 419–425.
22. Park, D. H., Kim, B. C., Kim, J. J. and Park, L. S., Effect of glass particle size on sintering behaviors of the glass–alumina composities for low firing temperature. *J. Korean Ceram. Soc.*, 2000, **37**, 545–551.
23. Kingery, W. D., Bowen, H. K. and Uhlmann, D. R., *Introduction to Ceramics* (*2nd ed.*). Wiley, New York, 1960, pp. 206–208.